

RESEARCH ARTICLE

Differentiation of human embryonic stem cells into corneal epithelial progenitor cells under defined conditions

Canwei Zhang^{1,2}, Liqun Du¹, Kunpeng Pang¹, Xinyi Wu^{1*}

1 Department of Ophthalmology, Qilu Hospital of Shandong University, Jinan, Shandong, PR China, **2** The Key Laboratory of Cardiovascular Remodeling and Function Research, Chinese Ministry of Education and Chinese Ministry of Health, Qilu Hospital of Shandong University, Jinan, Shandong, PR China

* xywu8868@163.com.



Abstract

The development of cell-based therapies using stem cells represents a significant breakthrough in the treatment of limbal stem cell deficiency (LSCD). The aim of this study was to develop a novel protocol to differentiate human embryonic stem cells (hESCs) into corneal epithelial progenitor cells (CEPCs), with similar features to primary cultured human limbal stem cells (LSCs), using a medium composed of DMEM/F12 and defined keratinocyte serum-free medium (KSFM) (1:1) under different carbon dioxide (CO₂) levels in culture. The differentiated cells exhibited a similar morphology to limbal stem cells under 5%, 7%, and 9% CO₂ and expressed the LSC markers ABCG-2 and p63; however, CK14 was only expressed in the cells cultured under 7% and 9% CO₂. Quantitative reverse-transcription polymerase chain reaction (RT-PCR) analysis indicated that the ABCG2, p63, and CK14 levels in the 7% CO₂ and 9% CO₂ groups were higher than those in the 5% CO₂ group and in undifferentiated hESCs ($p < 0.05$). The highest expression of ABCG2 and p63 was exhibited in the cells cultured under 7% CO₂ at day 6 of differentiation. Western blotting indicated that the ABCG2 and p63 levels were higher at day 6 than the other time points in the 7% CO₂ and 9% CO₂ groups. The highest protein expression of ABCG2 and p63 was identified in the 7% CO₂ group. The neural cell-specific marker tubulin β 3 and the epidermal marker K1/10 were also detected in the differentiated cells via immunofluorescent staining; thus, cell sorting was performed via fluorescence-activated cell sorting (FACS), and ABCG2-positive cells were isolated as CEPCs. The sorted cells formed three to four layers of epithelioid cells by airlifting culture and expressed ABCG2, p63, CK14, and CK3. In conclusion, the novel induction system conditioned by 7% CO₂ in this study may be an effective and feasible method for CEPC differentiation.

OPEN ACCESS

Citation: Zhang C, Du L, Pang K, Wu X (2017) Differentiation of human embryonic stem cells into corneal epithelial progenitor cells under defined conditions. PLoS ONE 12(8): e0183303. <https://doi.org/10.1371/journal.pone.0183303>

Editor: Wei Li, Xiamen University, CHINA

Received: December 18, 2016

Accepted: August 2, 2017

Published: August 15, 2017

Copyright: © 2017 Zhang et al. This is an open access article distributed under the terms of the [Creative Commons Attribution License](https://creativecommons.org/licenses/by/4.0/), which permits unrestricted use, distribution, and reproduction in any medium, provided the original author and source are credited.

Data Availability Statement: All relevant data are within the paper and its Supporting Information files.

Funding: This work was supported by the National Natural Science Fund of China (No. 81271716; <https://isisn.nsf.gov.cn/egrantindex/funcindex/prjsearch-list>) and Key research and development program of Shandong Province (No. 2015GGE27292; <http://www.sdsc.gov.cn/>). The funders had no role in study design, data collection and analysis, decision to publish, or preparation of the manuscript.

Introduction

Corneal epithelium is continuously renewed by the proliferation and differentiation of stem cells located in the basal layer of the limbus, and it plays an important role in maintaining a clear, healthy cornea and preserving vision [1,2]. Destruction or damage to limbal stem cells

Competing interests: The authors have declared that no competing interests exist.

(LSCs) may cause limbal stem cell deficiency (LSCD) and the consequent absence of an intact epithelial layer, in addition to conjunctival ingrowth, neovascularization, chronic inflammation, impaired vision, and ultimately blindness [3,4]. Currently, cultured limbal epithelium transplantation has presented very encouraging clinical results for LSCD treatment [5,6]. However, there are several limitations in the source of limbal tissues [7]. Moreover, the risks of LSCD development in the donor eye was also a controversial issue for the transplantation of autologous limbal epithelium [8]. The development of cell-based therapies using stem cells represents a significant breakthrough in the treatment of LSCD, thus providing a more rational, less invasive, and better physiological treatment option in regenerative medicine for the ocular surface [9].

Human embryonic stem cells (hESCs) possess the features of unlimited proliferation paired with an ability to differentiate into cells of all three embryonic germ layers [10,11]. Recently, hESCs have demonstrated their clinical value. They have substantial potential in cell replacement therapy and regenerative medicine [12,13].

Previous studies have indicated that hypercapnia may improve the conservation and proliferation of hematopoietic progenitors [14,15]. Culture in a 10% carbon dioxide (CO₂) environment results in a substantial enhancement in hamster eight-cell embryo development [16]. An enhanced differentiation particularly toward the mesodermal and endodermal lineages at cultures maintained and differentiated at lowered CO₂ levels has also been reported [17]. This finding indicates that changes in the CO₂ concentration for cell cultures may affect the growth and differentiation of stem cells. In our preliminary experiment, we determined that 7% CO₂ has beneficial effects on the differentiation of corneal epithelial progenitor cells (CEPCs) from hESCs. Therefore, in this study, three CO₂ concentrations (5%, 7%, and 9%) were selected to evaluate the differentiation efficiencies of CEPCs from hESCs. Collagen IV is a major basement membrane component of limbal and corneal epithelia [18,19]. Previous studies have shown that collagen IV may be used to differentiate mouse ESCs into CEPCs and provide a good substrate for the induction of LSCs from hESCs [20–22].

Differentiation of hESCs/induced pluripotent stem (iPS) cells into corneal epithelial cells or stem cells continues to pose a challenge because the growth factors and three-dimensional signals that control hESC differentiation have remained elusive [23]. Most previously published studies have relied on the use of undefined factors such as conditioned medium, PA6 feeder cells, Bowman's membrane, or amniotic membrane [20,21,24,25]. Recently, several studies have focused on the differentiation of corneal epithelial cells from iPS cells under defined conditions, such as differentiation medium [26], small molecule inhibitors (SB-505124 and IWP-2) in combination with FGF [27], or collagen IV together with keratinocyte culture medium [28]. The use of defined differentiation conditions, free from animal-derived components, would minimize the potential risk of animal pathogen transmission, immune reactions, and graft rejection. A defined condition would also improve the repeatability and consistency of differentiation [27]. However, the defined conditions to differentiate hESCs into CEPC are not available.

In this study, we developed a novel protocol to differentiate hESCs into CEPCs using collagen IV and a differentiation medium composed of DMEM/F12 and defined keratinocyte-serum free medium (KFSM) under 7% CO₂. This method has substantial potential to provide an infinite cell source of CEPCs, with similar phenotypic and functional characterization to LSCs, for basic biological research and LSCD treatment.

Materials and methods

Isolation and culture of hLSCs from human limbus tissue

LSCs were isolated from donor limbal rim, which was not suitable for transplantation, obtained from Qilu Hospital of Shandong University. All tissue collection complied with the

guidelines of the Helsinki Declaration and was approved by the Medical Ethics Committee of Qilu Hospital of Shandong University, China. Written informed consent was obtained from the donors or next of kin. LSCs were isolated and cultured as previously described [3]. Primary cells were seeded on plates coated with 2% growth factor reduced Matrigel (354230, BD Biosciences, San Jose, CA, USA). The culture medium (LM) consisted of DMEM/F12 and DMEM (1:1) with 1% penicillin-streptomycin, 10% fetal bovine serum, 10 ng/ml EGF, 5 mg/ml insulin, 0.4 µg/ml hydrocortisone, 10^{-10} M cholera toxin, and 2×10^{-9} M 3,3',5-triiodo-L-thyronine.

Culture of human embryonic stem cells

The hESC line employed was H1 (WiCell Research Institute Inc., Madison, WI, USA), which was grown on hES-qualified Matrigel (Corning®, Tewksbury, MA, USA) coated plates with mTeSR1 medium (STEMCELL Technologies, Vancouver, Canada) as previously described [29,30]. The cells were incubated at 37°C in a humidified atmosphere that contained 5% CO₂ and were passaged every 5 days.

Differentiation of corneal epithelial progenitor cells

hESCs were released from the culture using 1 mg/ml dispase and plated into six-well tissue culture plates coated with collagen IV. The cells were cultured in mTeSR1 for 2 days and subsequently transferred into three different incubators, in which the CO₂ concentration was 5%, 7%, and 9%, respectively; thus, the experimental groups were designated as 5% CO₂, 7% CO₂ and 9% CO₂. The medium was changed into KFSM-DMEM/F12 (KDM). The hESCs grew slowly on Collagen IV-coated plates in mTeSR1, and clone detachment appeared after 3 days of culture; thus, hESCs cultured on hES-qualified Matrigel coated plates with mTeSR1 were used as the controls. The medium was replaced every day.

Cell number counting

Cell number counting was performed to assess cell proliferation as previously described [31]. Briefly, hESCs were released from the culture and dispersed by gently pipetting up and down several times. The cells were then equally distributed into three groups (5% CO₂, 7% CO₂, and 9% CO₂), with approximately 20 cell aggregates per well of six-well plates. At days 3, 6, 9, and 12 of differentiation, the cells were detached from the culture dishes using a 0.05% trypsin and 0.5 mM EDTA solution, and 0.4% (w/v) Trypan blue solution (Solarbio, China) was subsequently added to the cell suspension. The cells excluding the dye were considered viable and counted on a hemocytometer under optical microscopy.

Immunofluorescent staining of cell cultures

Cells were fixed with 4% paraformaldehyde for 20 minutes and incubated in 0.5% Triton X-100 for 10 minutes and 5% goat serum for 30 minutes. The primary antibodies included mouse anti-ABCG2 (1:100; Abcam Technologies, Cambridge, UK), rabbit anti-p63 (1:100; Abcam Technologies, Cambridge, UK), rabbit anti-CK14 (1:100; Abcam Technologies, Cambridge, UK), mouse anti-CK3 (1:100; Santa Cruz Biotechnology, Santa Cruz, CA, USA), rabbit anti-Tubulin β3 (1:100; BioLegend, San Diego, CA, USA), mouse anti-CK1/10 (1:100; Santa Cruz Biotechnology, Santa Cruz, CA, USA) and rabbit anti-MITF (1:50; Sigma-Aldrich Corporation, St. Louis, MO). Cells were incubated with the primary antibodies overnight at 4°C. Secondary antibodies (1:100; all obtained from Beijing Zhongshan Technologies, Beijing, China) coupled to fluorescein isothiocyanate (FITC) or tetramethyl rhodamine isothiocyanate (TRITC) were subsequently applied for detection. The cells were then stained with 4, 6-diamidino-

2-phenylindole (DAPI) to visualize the nuclei. Fluorescence was observed using a fluorescence microscope (model BH2RFL-T3, Olympus Corporation, Tokyo, Japan).

Quantitative reverse-transcription polymerase chain reaction (qRT-PCR)

Total RNA was extracted from the differentiated cells with TRIzol reagent (Invitrogen Corporation, Carlsbad, CA, USA), and cDNA was synthesized with a First Strand cDNA Synthesis Kit (Toyobo, Osaka, Japan) according to the manufacturer's protocol. Then, qRT-PCR was performed in triplicate on a sequence detection system (ABI Prism 7000; Life Technologies/Applied Biosystems, Inc., Foster City, CA, USA). The mean CT values were calculated, and the relative expression values were calculated from the delta CT values using the formula: $2^{-\Delta\Delta CT}$. The volume of RT-PCR was 20 μ l, including 2 μ l cDNA, 10 μ l SYBR Green Real-time PCR Master Mix (Toyobo, Osaka, Japan), 1 μ l each of specific forward and reverse primers, and 6 μ l sterile water. Quantitative RT-PCRs were run in duplicate using a LightCycler (Roche, Basel, Switzerland) at 95°C for 30 seconds, followed by 40 cycles of 95°C for 5 seconds, 56–60°C for 10 seconds, and 72°C for 60 seconds. The primers used were as follows: ABCG2, forward 5' – ACGAACGGATTAAACAGGGTCA – 3' ; and reverse 5' – CTCCAGACACACCACGGAT – 3' ; P63a, forward 5' – TGCCAGACTCAATTTAGTGA – 3' ; and reverse 5' – GAGGAGCCGTTCTGAATCTG – 3' ; CK14, forward 5' – TCCTTCGCACCAAGAACTGAG – 3' ; and reverse 5' – CAGGAGAGGGGATCTTCCAGT – 3' ; CK3, forward 5' – GGATGTGGACAGTGCCTATATG – 3' ; and reverse 5' – AGCGTCGTAGAGGGTCTT – 3' ; OCT4, forward 5' – CAAAGCAGAAACCC TCGTGC – 3' ; and reverse 5' – TCTCACTCGGTTCTCGATACTG – 3' ; GAPDH, forward 5' – TGAACGGGAAGCTCACTGG – 3' ; and reverse 5' – TCCACCACCCTGTTGCTGTA – 3' . For the normalization of the gene expression levels, the gene-to-GAPDH (housekeeping gene) was calculated and compared to that of the undifferentiated hESCs. LightCycler software and LightCycler Relative Quantification software were used to analyze the data.

Western blot analysis

Western blotting proceeded as previously described [32]. Briefly, cells were collected and lysed by shaking at 4°C for 30 minutes in RIPA buffer that contained protease inhibitors. The cell lysates were centrifuged at 12,000 g for 15 minutes at 4°C. The supernatant was boiled for 10 minutes. The total protein was quantified, and the protein samples were subjected to 10% sodium dodecyl sulfate-polyacrylamide gel electrophoresis (SDS-PAGE) and subsequently transferred to nitrocellulose membranes. The membranes were blocked with 5% skim milk in Tris-buffered saline for 2 hours at room temperature prior to overnight incubation at 4°C with primary antibodies, washed with Tris-buffered saline and incubated with secondary antibodies for 2 hours at 37°C. Protein bands were visualized using enhanced chemiluminescence as described by the supplier. A densitometric analysis was conducted with Quantity One software (Bio-Rad Laboratories, Berkeley, CA, USA).

Fluorescence-activated cell sorting (FACS) analysis and purification

The cell sorting analysis and purification were performed as previously reported [23,33]. The differentiated cells were digested using trypLE™ Express (Gibco, Thermo Fisher Scientific, Waltham, MA, USA) for 10 minutes at 37°C and then incubated with PerCP-Cy™5.5 Mouse anti-ABCG2 antibody (1:20, BD Technologies, Durham, NC, USA) in complete DMEM/F12 medium for 30 minutes at 4°C. The cells were washed three times with ice-cold phosphate buffered saline (PBS) prior to analysis using a Guava® easyCyte™ cytometer (Millipore Technologies, Billerica, MA, USA). The negative controls included isotype-matched irrelevant

antibodies. Cell isolation was conducted on a FACS Aria II (BD Biosciences, San Jose, CA, USA).

Airlifting culture

CEPCs were gently seeded at $1.5 \times 10^4 \text{ mm}^{-2}$ on the Bowman's membrane side of acellular porcine limbal matrix (APLM) prepared as previously described [34–36]. The cells were cultured in a submerged condition for 7 days and subsequently changed to air-lift culture for an additional 7 days to induce epithelial stratification [20]. The medium was LM and changed daily during airlifting.

Histology

The epithelial sheets were fixed and processed, embedded into paraffin blocks and mounted as 4- μm -thick paraffin-embedded sections. Hematoxylin and eosin (HE) staining was performed using conventional methods. For immunohistochemical analyses, deparaffinized sections were treated with a primary antibody at 4°C overnight and subsequently incubated with secondary antibodies conjugated with FITC or TRITC in the dark for 1 hour at room temperature. The primary and secondary antibodies were the same as those used in immunocytochemistry. Fluorescence was observed under a fluorescence microscope. For western blotting and qRT-PCR, the cell sheets were snap frozen in liquid nitrogen and grinded to powder using a pre-cooled pestle; hESCs seeded on APLM were used as the control. The subsequent steps were similar to those of the previously described cells.

Statistical analysis

All statistical analyses were performed using SPSS 13.0. Data are presented as the mean \pm standard deviation. The t-test and One-way analysis of variance (ANOVA) were used for statistical analysis. Differences were considered statistically significant at $p < 0.05$.

Results

Isolation, culture, and identification of hLSCs

Human LSCs were successfully isolated from human limbal tissue and cultured in feeder-free cell culture conditions as previously reported [2]. The cells were small and cuboidal and exhibited the expression of the LSC markers ABCG2, p63, and CK14, similar to previous reports [2,37] (Fig 1B).

Morphological changes and proliferation capacity of differentiated hESCs

Within the first 3 days of differentiation, the cells became relatively flatter and spread out appearing under 7% CO₂. On day 6, the majority of the cells changed into small cuboid cells and formed regularly arranged, cobble stone-like cell sheets, similar to primary cultured LSCs. On day 9, the number of cells increased, and nearly all cells exhibited a cobble stone-like morphology. On day 12, the cells became much flatter, and the cells with an increased cell size appeared in the periphery (Fig 1C). A similar morphological change was identified in the cells cultured under 5% and 9% CO₂; however, the cells under 5% CO₂ were much flatter and grew more slowly than the cells cultured under 7% CO₂ and 9% CO₂ (Fig 1C). To define the cell growth in the three groups, cell number counting was performed. Trypan blue dyed cell counting showed that the cell density in the cultures under 5% CO₂ was significantly lower than that in the cultures under 7% CO₂ and 9% CO₂ on days 9 and 12 ($p < 0.05$) (Fig 2).

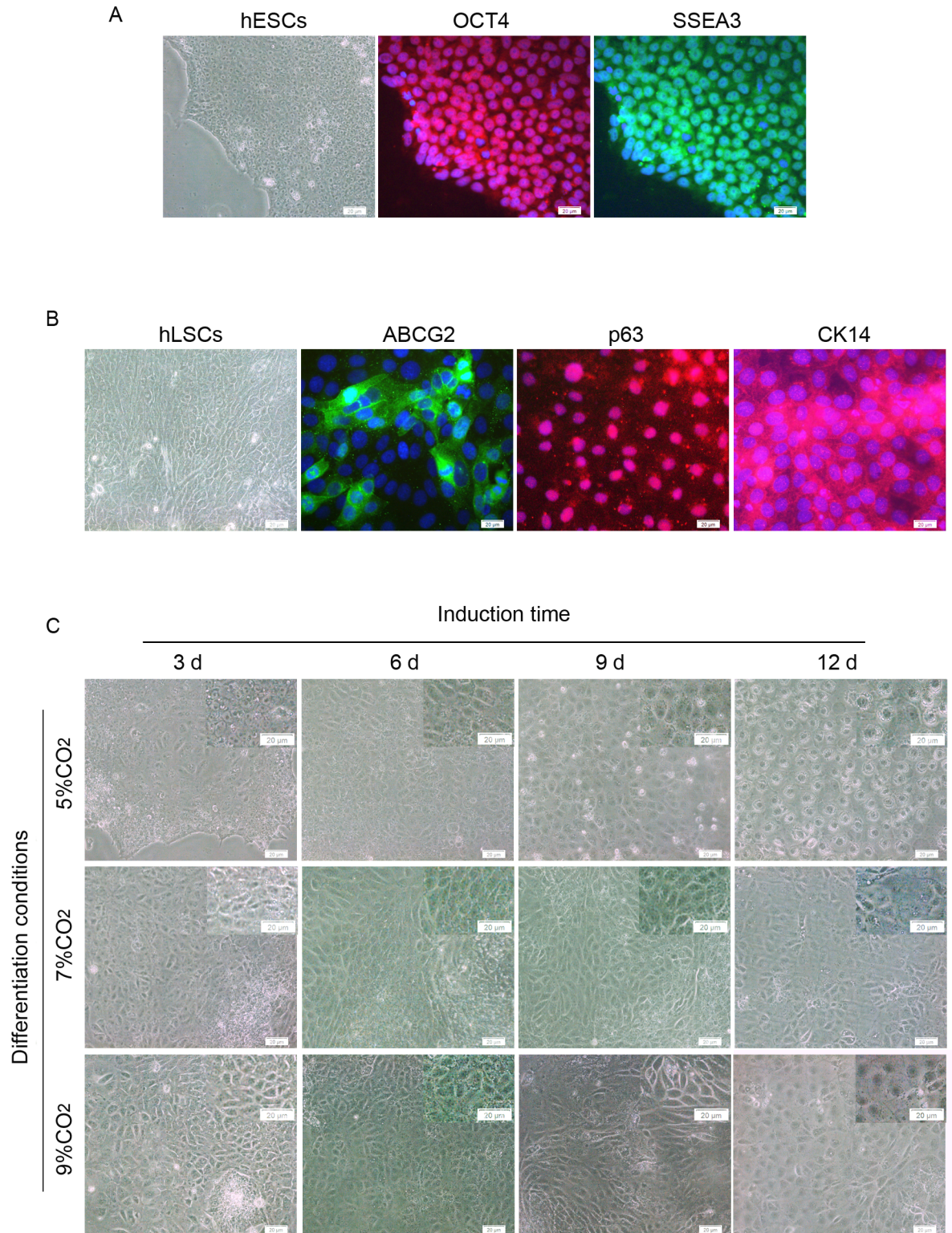


Fig 1. Primary cultured hLSCs and morphology of cells from hESCs at different stages of differentiation. (A) Microscopic image of hESCs and the expression of OCT4 and SSEA-3. (B) Morphology of hLSCs and immunofluorescent staining of ABCG2, p63, and CK14. (C) Representative images of the differentiated cells at days 3, 6, 9, and 12 of differentiation. Scale bar, 20 μ m.

<https://doi.org/10.1371/journal.pone.0183303.g001>

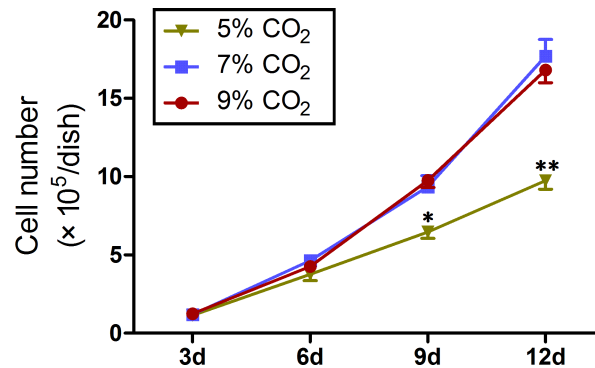


Fig 2. Number of cells counted using a hemocytometer. Data represent mean \pm SD of three independent experiments with triplicate dishes.

<https://doi.org/10.1371/journal.pone.0183303.g002>

Differentiation of hESCs into CEPs

The differentiation of hESCs into CEPs was confirmed via immunofluorescence, qRT-PCR analysis, and western blotting. The immunofluorescence of the fixed cells showed that the expression of ABCG2, p63, and CK14, which are the markers for LSCs [26,38,39], were strongly expressed in the cytomembrane, nucleus, and cytoplasm of the induced cells under 7% and 9% CO₂, respectively. CK3, the terminally differentiated cell marker, which is specific to corneal epithelium [40,41], was also identified at the periphery of some colonies on day 12 of differentiation (Fig 3B and 3C). However, the immunofluorescence signals of CK14 could not be detected in the cells cultured under 5% CO₂, and the expression of ABCG2 and CK3 was also very weak in these cells (Fig 3A). These data indicate that hESCs cultured on collagen IV in KSFM-DMEM/F12 may be differentiated into CEPs, and a slightly elevated CO₂ level is more conducive to the differentiation of CEPs from hESCs. The expression of CK3 demonstrated that this culture condition may not be helpful in the maintenance of stem cell properties, and the cells at the periphery of some colonies can further differentiate into corneal epithelial cells.

Quantitative RT-PCR analysis was performed to confirm the differentiation of hESCs into CEPs. In all three groups, the expression of p63 began to increase on day 3 (Fig 4B). In the 7% CO₂ and 9% CO₂ groups, but not in the 5% CO₂ group, the expression of ABCG2 and CK14 exhibited a significant increase on day 3 (Fig 4A and 4C). The ABCG2, p63, and CK14 levels peaked at the 6-day time point in the 7% CO₂ and 9% CO₂ groups. The highest expression of ABCG2 (averaged 21.65-fold), p63 (averaged 30.01-fold), and CK14 (averaged 16.07-fold) was identified in the 7% CO₂ group. However, we did not identify significant differences in the levels of ABCG2, p63, and CK14 between the 7% CO₂ group and the 9% CO₂ group. The expression of CK3 was elevated in all experimental groups on days 9 and 12 (Fig 4D). The upregulation of CK3 accompanied with decreased expression of ABCG2, p63, and CK14 decreased in the 7% CO₂ and 9% CO₂ groups, which suggests that corneal epithelial differentiation may be in progress. OCT4, a marker of undifferentiated hESCs, is crucial to the establishment of pluripotential identity [42]. In all experimental groups, the expression of OCT4 significantly decreased within 6 days of differentiation and declined to nearly negligible levels by day 12 (Fig 4E). These findings suggested that there was a loss of hESC pluripotency during the differentiation process.

The differentiated cells under 7% and 9% CO₂ were used to analyze the changes in the ABCG2, p63, CK14, CK3, and OCT4 protein levels during the differentiation process because the expression of ABCG2, CK14, and CK3 could not be detected in the 5% CO₂ group via

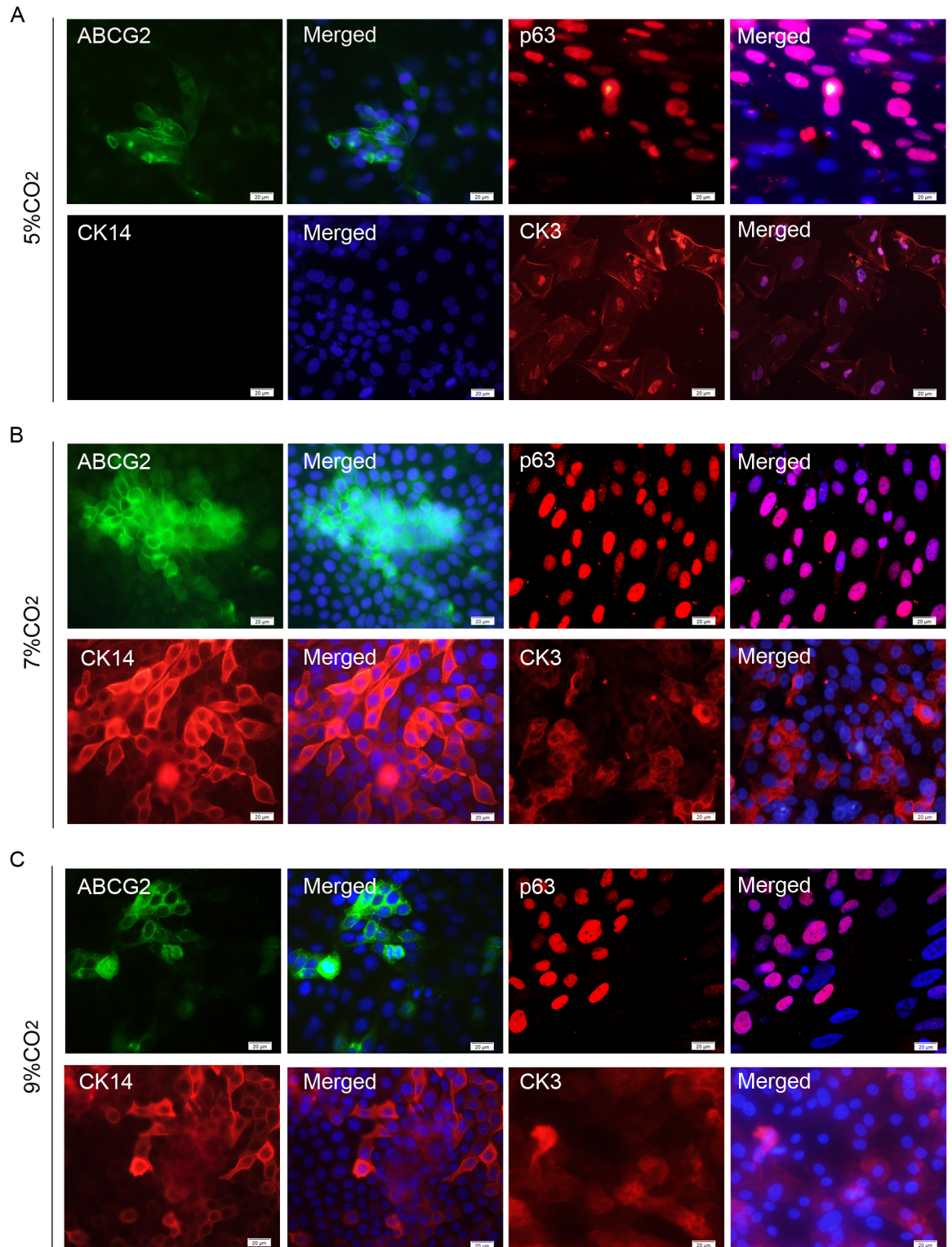


Fig 3. Immunofluorescence images of the differentiated cells. Expression of ABCG2, p63, and CK14 at day 6 and CK3 at day 12 of differentiation in the cells cultured under 5% CO₂ (A), 7% CO₂ (B), and 9% CO₂ (C). Scale bar, 20 μm.

<https://doi.org/10.1371/journal.pone.0183303.g003>

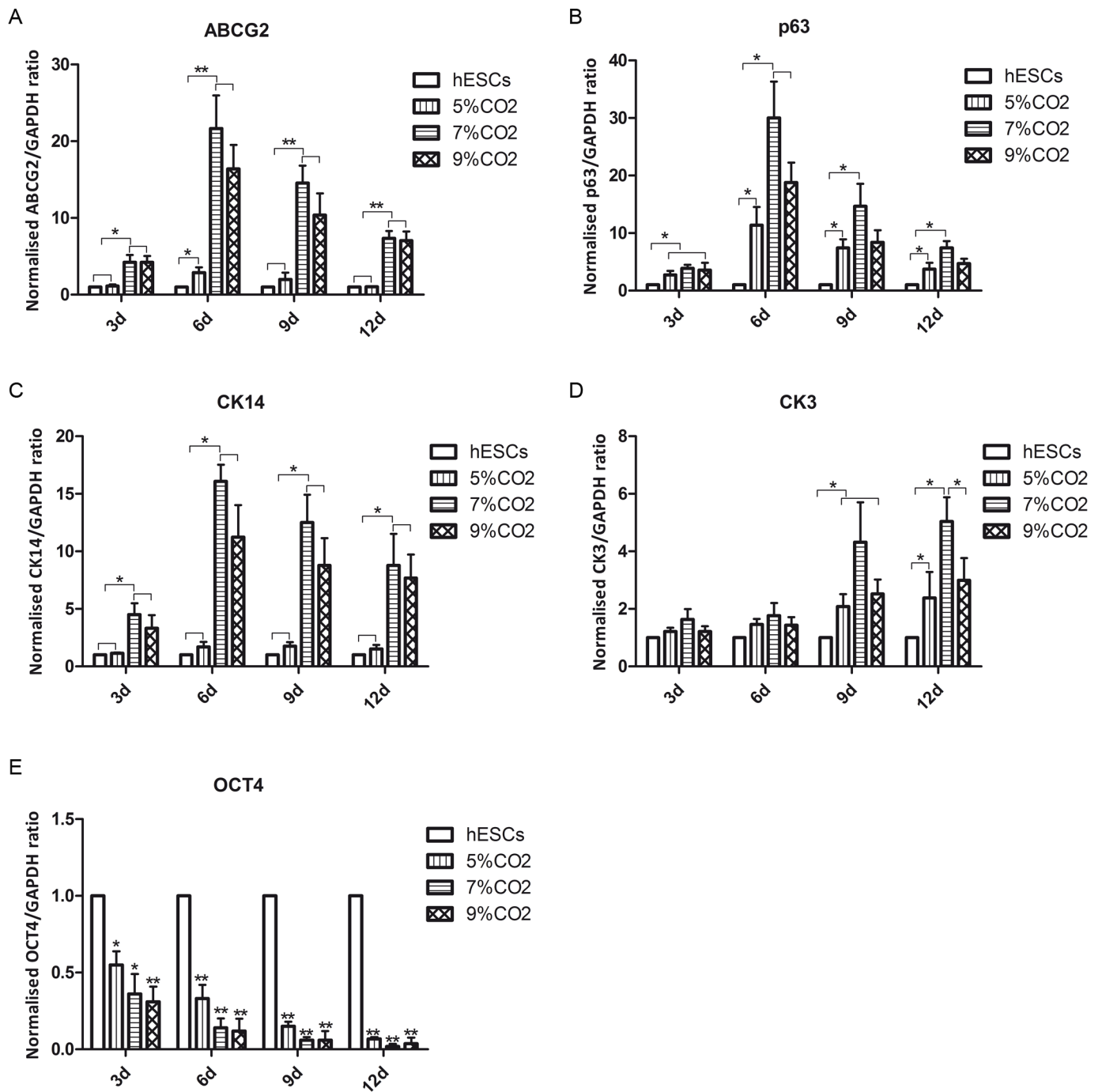


Fig 4. Time course of ABCG-2, p63, CK14, and CK3 during hESC differentiation culture (3, 6, 9, and 12 days). Data are representative of three experiments and presented as the mean \pm SD. * $p < 0.05$, ** $p < 0.01$.

<https://doi.org/10.1371/journal.pone.0183303.g004>

western blotting. The results showed that the ABCG2, p63, and CK14 levels increased within 6 days of differentiation and declined at day 9. CK3 was detected in both groups at day 9; however, both bands were very weak (Fig 5A and 5B). Moreover, the expression of ABCG2, p63, and CK14 in the 7% CO₂ group was higher than that in the other groups (Fig 5C).

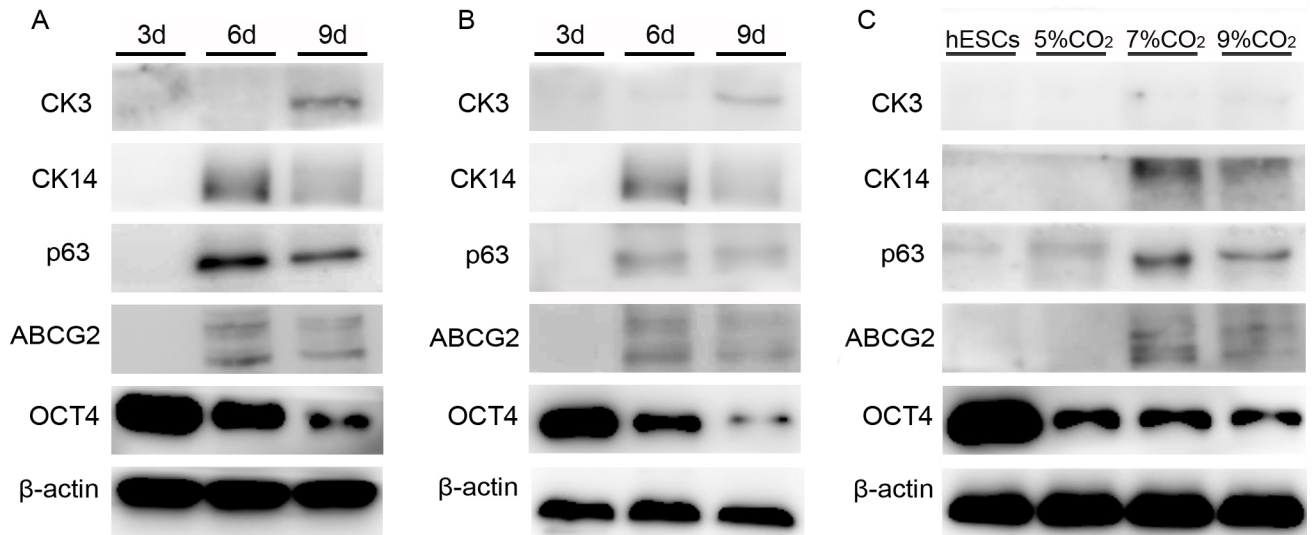


Fig 5. Protein expression of CEPC and hESC markers at different time points and in different culture conditions. (A-B) ABCG2, p63, CK14, CK3, and OCT4 protein expression in the 7% CO₂ (A) and 9% CO₂ (B) groups at different time points (3, 6, and 9 days). (C) Protein level of ABCG2, p63, CK14, CK3, and OCT4 at 5%, 7%, and 9% CO₂ at day 6 of differentiation. The undifferentiated hESCs were used as the control group.

<https://doi.org/10.1371/journal.pone.0183303.g005>

Investigation of non-corneal epithelial cell lineages and isolation of CEPCs derived from hESCs

We determined that the differentiated cells could form identifiable different zones in larger clones, similar to previous report [26]; thus, the derivation of non-corneal epithelial cells was examined via immunofluorescence. The neural cell-specific marker tubulin β3, the epidermal marker K1/10, and the retinal pigment epithelial cell marker MITF were investigated (Fig 6A). The immunofluorescent signal of tubulin β3 was detected in the center of some larger clones; however, it could not be detected in the small clones. CK1/10 was also identified at the periphery of a small number of clones on the 12th day of differentiation; however, MITF was not detected in the cultures. These findings indicate the presence of neural cell-like and epidermal cell-like cells in the differentiated cells; thus, the cell sorting was performed by FACS. ABCG2 is strictly confined to small clusters of basal cells in the limbal epithelium and may provide a suitable tool for the identification of human limbal stem cells (hLSCs) [43,44]; thus, ABCG2--positive cells were isolated by FACS. The data showed that the number of ABCG2-positive cells in the 7% CO₂ group was significantly higher than that in the other groups, with an average of 27.41% of cells expressing ABCG2 at day 6 of differentiation (Fig 6B). The sorted cells were seeded on the plates coated with 2% growth factor reduced Matrigel as previously described. The expression of ABCG2, p63, and CK14, but not CK3, CK1/10, and tubulin β3, was detected in the cells via immunofluorescence (Fig 6C).

Airlifting culture of CEPCs

By airlifting culture on APLM, CEPCs formed stratified and closely arranged epithelioid cell sheets that consisted of three to four layers of elongated cells (Fig 7B). ABCG2, p63, CK14, and CK3 were detected in the epithelioid cell sheets via immunofluorescence; however, p63 was only expressed in some basal cells. CK1/10 and tubulin β3 were not identified in these cells by immunofluorescence (Fig 7C–7H). Quantitative RT-PCR analysis indicated that the ABCG2,

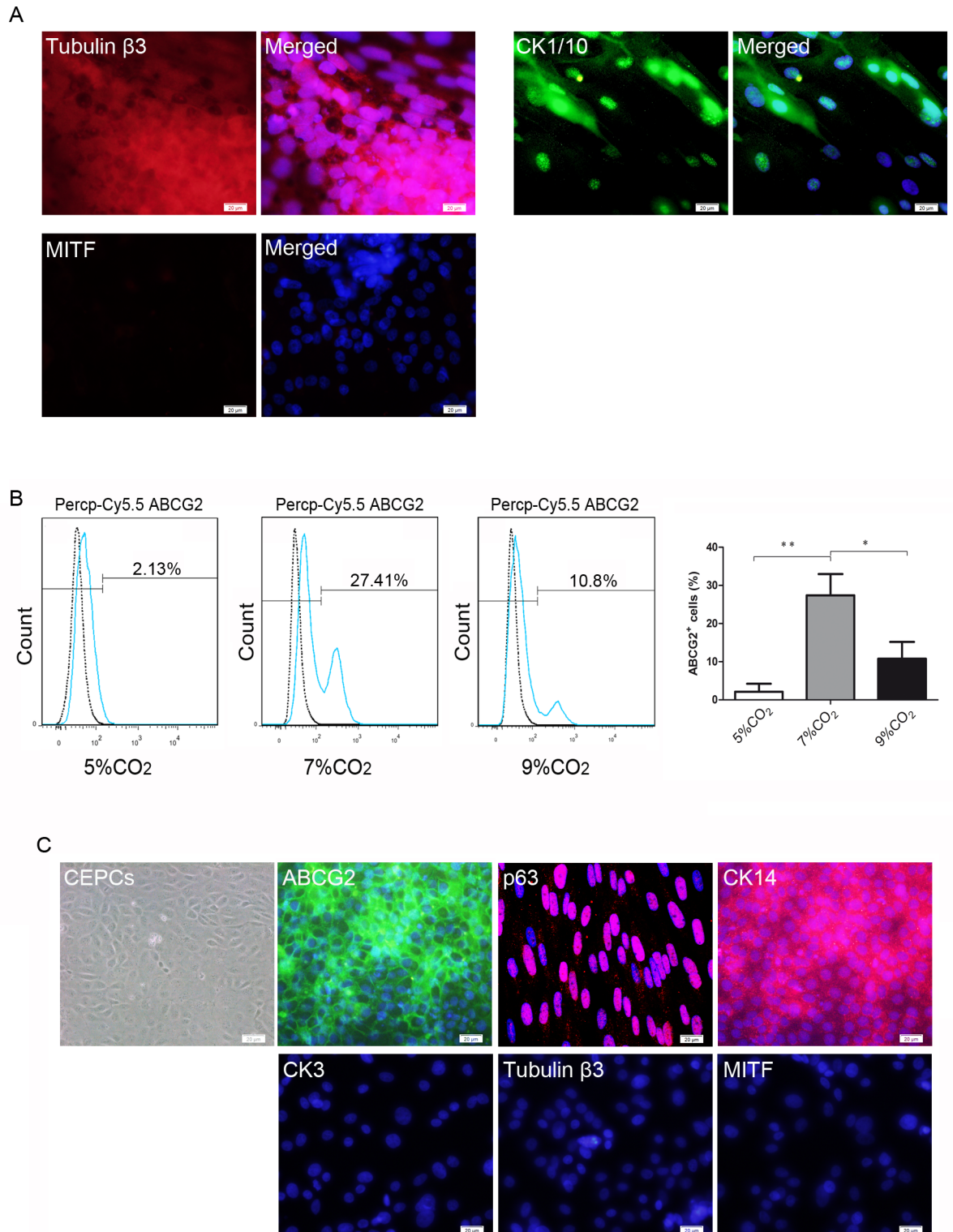


Fig 6. Immunostaining of non-corneal epithelial differentiation markers and isolation of CEPCCs derived from hESCs by FACS. (A) Immunofluorescent staining of tubulin β 3, CK1/10, and MITF. (B) FACS analysis of ABCG2-positive cells in different culture conditions at day 6 of differentiation. (C) Immunofluorescent staining of the sorted cells. ABCG2, p63, and CK14 were strongly expressed in the sorted cells. CK3, tubulin β 3, and CK1/10 were not detected. Scale bar, 20 μ m.

<https://doi.org/10.1371/journal.pone.0183303.g006>

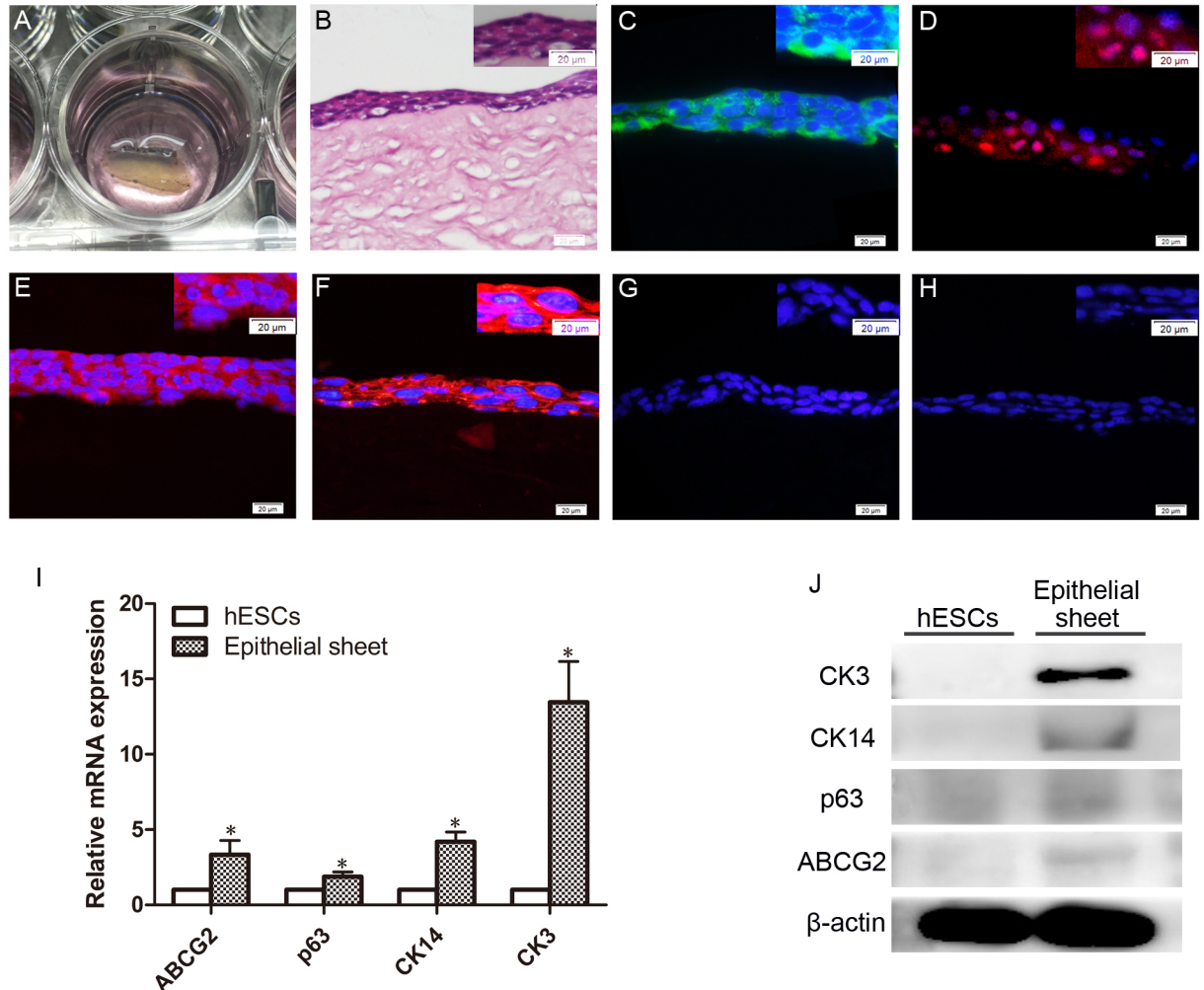


Fig 7. Characterization of epitheloid cell sheet on APLM. (A) Epitheloid cell sheets under airlifting culture. (B) HE staining of epitheloid cell sheet. (C-G) Immunofluorescent staining of ABCG2 (C), p63 (D), CK14 (E), CK3 (F), tubulin β3 (G), and CK1/10 (H) in the cells cultured on APLM. Scale bar, 20 μm. (I-J) Gene (I) and protein (J) expression of ABCG2, p63, CK14, and CK3 in epitheloid cell sheets. hESCs seeded on APLM were used as the control. Data are representative of three experiments and presented as the mean ± SD. *p < 0.05, **p < 0.01.

<https://doi.org/10.1371/journal.pone.0183303.g007>

p63, CK14, and CK3 levels in the epithelial sheets were significantly higher than those of the hESCs seeded on APLM (Fig 7I). However, p63 was not detected by western blotting, and the expression of ABCG2 and CK14 was very low in the epithelial sheets (Fig 7J). We suggest this may be caused by further differentiation of CEPs into corneal epithelial cells on APLM.

Discussion

In the present study, we established an effective and feasible strategy for the differentiation of CEPs from hESCs *in vitro* under defined conditions. The sorted cells express the LSC markers ABCG2, p63, and CK14 and form stratified epitheloid cell sheets. These findings suggest that the differentiated cells have similar features to primary cultured hLSCs. Moreover, the protocol we developed provides a novel insight, other than mimicking the microenvironment of LSCs, into the differentiation of CEPs.

During the differentiation process, we found the identifiable different zones in some large clones; however, most of the cells displayed an epithelial cell-like morphology and expressed corneal epithelial stem cell markers. FACS indicated that an average of 27.41% of the cells were ABCG2-positive. Therefore, cell sorting must be performed for the purification of CEPCs. CK14 and p63, but not CK3, CK1/10, and tubulin β 3, were also detected in the sorted cells, which suggests that CEPCs of high purity could be attained in this protocol through cell sorting.

KSFM is a type of optimized medium used to support the growth and expansion of human keratinocytes, corneal epithelial cells, and LSCs [45–49]. Trans-membrane cadherins played an important role in the early-stage differentiation of hESCs, particularly in the differentiation of the ectoderm [50,51]. KSFM, mixed with DMEM/F12, increased its calcium concentration, which may facilitate the differentiation of ectodermal cells from hESCs. The expression of ABCG2, p63, CK14, CK3, CK1/10, and tubulin β 3 in the differentiated cells demonstrated that hESCs cultured in KSFM-DMEM/F12 could differentiate into epithelial progenitor cells, including CEPCs. Furthermore, the feature of KSFM that facilitates epithelial or epithelial precursor cell growth may also be an important factor in the differentiation of CECs from hESCs. However, the explicit mechanisms require intensive study.

The expression of ABCG2, p63, and CK14 decreased at day 9 compared with day 6 of differentiation, whereas the CK3 levels started to increase in our studies, which suggested that this culture system could not serve as the niche in the long-term maintenance of LSC properties, and corneal epithelial differentiation had progressed further during the differentiation. These findings also indicated that the 6th day of differentiation may be a suitable time to perform cell sorting of CEPCs from cultures in this differentiation model. The expression of CEPC markers, particularly ABCG2 and CK14, was substantially higher in the differentiated cells under 7% CO₂ than that under 5% CO₂, which indicates that slightly elevated CO₂ was conducive to the differentiation of CEPCs from hESCs. However, the involved mechanism remained unclear. Previous studies have indicated that elevated CO₂ enhances embryo development by its action as a weak acid to maintain the appropriate intracellular pH [16]. Moreover, hypercapnia caused nuclear translocation of IKK α , and IKK α is implicated in the differentiation of epithelial cells [52,53]. We speculate these factors may play roles in the differentiation of CEPCs from hESCs. The invasive ability of colon cancer cells increased under hypercapnic conditions [54], and elevated levels of CO₂ are favored for the enhanced proliferation of bone marrow (BM) progenitor cells [55]. Similar to previous reports, in this study, we determined that the cell density in the cultures under 7% and 9% CO₂ was higher than 5% CO₂ on the 9th and 12th days of differentiation, which indicated that slightly elevated levels of CO₂ may promote the proliferation of differentiated hESCs.

APLM and the limbal microvascular net play important roles as components of the limbal epithelial stem cell niche in the avoidance of the differentiation of limbal epithelial stem cells [24,56]. Our previous studies [35,36] have indicated that acellular porcine corneal matrix developed by sodium dodecyl sulfate (SDS) maintained the intact basement membrane and possessed good biocompatibility. The cells could form three to four layers of epithelioid cells on APLM by airlifting culture, and CK3 was detected in most cells; however, the expression of corneal epithelial stem cell markers, ABCG2 and p63, was very low. These data demonstrated that APLM without the limbal microvascular net could not maintain the limbal epithelial stem cell stemness. CEPCs derived from hESCs could generate corneal epithelial-like cells, which suggests that the cells seeded in a suitable corneal epithelial stem cell niche may be used in corneal tissue engineering or the treatment of LSCD. However, the derivation of ES cells from the human embryo raises ethical questions, in part because the predominant methods used require destruction of the embryo. Compared with ESCs, induced pluripotent stem (iPS) cells avoid ethical issues and may

be propagated as autologous cells without immunological rejection after transplantation [57]. Previous studies have indicated that iPS cells functionally equivalent to ESCs can generate cell types from each of the three embryonic germ layers: the endoderm, mesoderm and ectoderm [58,59]. We conclude that the differentiation method in this study may also be suitable for the derivation of epithelial lineage or corneal epithelial lineage from iPS cells.

Conclusions

In summary, we developed a novel protocol, which differs from mimicking the CEPC niche, to differentiate hESCs into CEPCs, and the differentiated cells exhibited similar morphological features, cell markers, and differentiation capacity as hLSCs. This differentiation model may provide a new step toward fully defined and xeno-free differentiation protocols to produce CEPCs for investigations of basic biology. Moreover, with the improvement of the cell sorting technique and the emergence of CEPC-specific markers, these differentiated cells hold substantial promise in regenerative medicine.

Supporting information

S1 File. The data of qRT-PCR.

(ZIP)

S2 File. The FACS analysis results of ABCG2-positive cells.

(ZIP)

Acknowledgments

The authors would like to thank Dr. Jing Zhu for guidance regarding human embryonic stem cell culture technology. This work was supported by the National Natural Science Fund of China (No. 81271716) and the Key research and development program of Shandong Province, People's Republic of China (No. 2015GGE27292).

Author Contributions

Conceptualization: Canwei Zhang, Xinyi Wu.

Data curation: Canwei Zhang, Liqun Du, Kunpeng Pang.

Formal analysis: Canwei Zhang, Liqun Du, Kunpeng Pang, Xinyi Wu.

Funding acquisition: Xinyi Wu.

Investigation: Canwei Zhang, Liqun Du, Kunpeng Pang.

Methodology: Canwei Zhang, Liqun Du, Xinyi Wu.

Project administration: Canwei Zhang, Xinyi Wu.

Resources: Xinyi Wu.

Supervision: Xinyi Wu.

Validation: Canwei Zhang, Liqun Du, Kunpeng Pang, Xinyi Wu.

Visualization: Canwei Zhang, Liqun Du, Kunpeng Pang, Xinyi Wu.

Writing – original draft: Canwei Zhang, Liqun Du.

Writing – review & editing: Liqun Du, Kunpeng Pang, Xinyi Wu.

References

1. Bettahi I, Sun H, Gao N, Wang F, Mi X, Chen W, et al. (2014) Genome-wide transcriptional analysis of differentially expressed genes in diabetic, healing corneal epithelial cells: hyperglycemia-suppressed TGFbeta3 expression contributes to the delay of epithelial wound healing in diabetic corneas. *Diabetes* 63: 715–727. <https://doi.org/10.2337/db13-1260> PMID: 24306208
2. Tsui S, Wang J, Wang L, Dai W, Lu L. (2016) CTCF-Mediated and Pax6-Associated Gene Expression in Corneal Epithelial Cell-Specific Differentiation. *PLoS One*. 2016 11:e0162071. <https://doi.org/10.1371/journal.pone.0162071> PMID: 27583466
3. Ouyang H, Xue Y, Lin Y, Zhang X, Xi L, Patel S, et al. (2014) WNT7A and PAX6 define corneal epithelium homeostasis and pathogenesis. *Nature* 511: 358–361. <https://doi.org/10.1038/nature13465> PMID: 25030175
4. Ksander BR, Kolovou PE, Wilson BJ, Saab KR, Guo Q, Ma J, et al. (2014) ABCB5 is a limbal stem cell gene required for corneal development and repair. *Nature* 511: 353–357. <https://doi.org/10.1038/nature13426> PMID: 25030174
5. Pedrotti E, Passilongo M, Fasolo A, Nubile M, Parisi G, Mastropasqua R, et al. (2015) In Vivo Confocal Microscopy 1 Year after Autologous Cultured Limbal Stem Cell Grafts. *Ophthalmology* 122: 1660–1668. <https://doi.org/10.1016/j.ophtha.2015.04.004> PMID: 26050542
6. Rama P, Matuska S, Paganoni G, Spinelli A, De Luca M, Pellegrini G. (2010) Limbal stem-cell therapy and long-term corneal regeneration. *N Engl J Med* 363: 147–155. <https://doi.org/10.1056/NEJMoa0905955> PMID: 20573916
7. Mikhailova A, Ilmarinen T, Ratnayake A, Petrovski G, Uusitalo H, Skottman H, et al. (2016) Human pluripotent stem cell-derived limbal epithelial stem cells on bioengineered matrices for corneal reconstruction. *Exp Eye Res* 146:26–34. <https://doi.org/10.1016/j.exer.2015.11.021> PMID: 26658714
8. Holland EJ, Schwartz GS. (2000) Changing concepts in the management of severe ocular surface disease over twenty-five years. *Cornea* 19:688–98. PMID: 11009321
9. Casaroli-Marano RP, Nieto-Nicolau N, Martinez-Conesa EM, Edel M, BA-P A (2015) Potential Role of Induced Pluripotent Stem Cells (iPSCs) for Cell-Based Therapy of the Ocular Surface. *J Clin Med* 4: 318–342. <https://doi.org/10.3390/jcm4020318> PMID: 26239129
10. Thomson JA, Itskovitz-Eldor J, Shapiro SS, Waknitz MA, Swiergiel JJ, Marshall VS, et al. (1998) Embryonic stem cell lines derived from human blastocysts. *Science* 282: 1145–1147. PMID: 9804556
11. Takahashi K, Tanabe K, Ohnuki M, Narita M, Ichisaka T, Tomoda K, et al. (2007) Induction of pluripotent stem cells from adult human fibroblasts by defined factors. *Cell* 131: 861–872. <https://doi.org/10.1016/j.cell.2007.11.019> PMID: 18035408
12. Schwartz SD, Hubschman JP, Heilwell G, Franco-Cardenas V, Pan CK, Ostrick RM, et al. (2012) Embryonic stem cell trials for macular degeneration: a preliminary report. *Lancet* 379: 713–720. [https://doi.org/10.1016/S0140-6736\(12\)60028-2](https://doi.org/10.1016/S0140-6736(12)60028-2) PMID: 22281388
13. Menasche P, Vanneau V, Hagege A, Bel A, Cholley B, Cacciapuoti I, et al. (2015) Human embryonic stem cell-derived cardiac progenitors for severe heart failure treatment: first clinical case report. *Eur Heart J* 36: 2011–2017. <https://doi.org/10.1093/eurheartj/ehv189> PMID: 25990469
14. Jeanne M, Kovacevic-Filipovic M, Szyporta M, Vlaski M, Hermitte F, Lafarge X, et al. (2009) Low-oxygen and high-carbon-dioxide atmosphere improves the conservation of hematopoietic progenitors in hypothermia. *Transfusion* 49: 1738–1746. <https://doi.org/10.1111/j.1537-2995.2009.02191.x> PMID: 19413727
15. Hamad M, Irhimeh MR, Abbas A (2016) Hypercapnia slows down proliferation and apoptosis of human bone marrow promyeloblasts. *Bioprocess Biosyst Eng* 39: 1465–1475. <https://doi.org/10.1007/s00449-016-1624-7> PMID: 27194031
16. Carney EW, Bavister BD (1987) Regulation of hamster embryo development in vitro by carbon dioxide. *Biol Reprod* 36: 1155–1163. PMID: 3113499
17. Jyoti S, Tandon S (2014) Hypocapnia leads to enhanced expression of pluripotency and meso-endo-dermal differentiation genes in mouse embryonic stem cells. *Exp Cell Res* 322: 389–401. <https://doi.org/10.1016/j.yexcr.2014.02.008> PMID: 24560741
18. Ljubimov AV, Burgeson RE, Butkowski RJ, Michael AF, Sun TT, Kenney MC. (1995) Human corneal basement membrane heterogeneity: topographical differences in the expression of type IV collagen and laminin isoforms. *Lab Invest* 72: 461–473. PMID: 7723285
19. Ihanamaki T, Pelliniemi LJ, Vuorio E (2004) Collagens and collagen-related matrix components in the human and mouse eye. *Prog Retin Eye Res* 23: 403–434. <https://doi.org/10.1016/j.preteyeres.2004.04.002> PMID: 15219875

20. Zhu J, Zhang K, Sun Y, Gao X, Li Y, Chen Z, et al. (2013) Reconstruction of functional ocular surface by acellular porcine cornea matrix scaffold and limbal stem cells derived from human embryonic stem cells. *Tissue Eng Part A* 19: 2412–2425. <https://doi.org/10.1089/ten.TEA.2013.0097> PMID: 23675636
21. Ahmad S, Stewart R, Yung S, Kolli S, Armstrong L, Stojkovic M, et al. (2007) Differentiation of human embryonic stem cells into corneal epithelial-like cells by in vitro replication of the corneal epithelial stem cell niche. *Stem Cells* 25: 1145–1155. <https://doi.org/10.1634/stemcells.2006-0516> PMID: 17255521
22. Homma R, Yoshikawa H, Takeno M, Kurokawa MS, Masuda C, Takada E, et al. (2004) Induction of epithelial progenitors in vitro from mouse embryonic stem cells and application for reconstruction of damaged cornea in mice. *Invest Ophthalmol Vis Sci* 45: 4320–4326. <https://doi.org/10.1167/iovs.04-0044> PMID: 15557438
23. Zhang K, Pang K, Wu X (2014) Isolation and transplantation of corneal endothelial cell-like cells derived from in-vitro-differentiated human embryonic stem cells. *Stem Cells Dev* 23: 1340–1354. <https://doi.org/10.1089/scd.2013.0510> PMID: 24499373
24. Hanson C, Hardarson T, Ellerstrom C, Nordberg M, Caisander G, Rao M, et al. (2013) Transplantation of human embryonic stem cells onto a partially wounded human cornea in vitro. *Acta Ophthalmol* 91: 127–130. <https://doi.org/10.1111/j.1755-3768.2011.02358.x> PMID: 22280565
25. Hayashi R, Ishikawa Y, Ito M, Kageyama T, Takashiba K, Fujioka T, et al. (2012) Generation of corneal epithelial cells from induced pluripotent stem cells derived from human dermal fibroblast and corneal limbal epithelium. *PLoS One* 7: e45435. <https://doi.org/10.1371/journal.pone.0045435> PMID: 23029008
26. Hayashi R, Ishikawa Y, Sasamoto Y, Katori R, Nomura N, Ichikawa T, et al. (2016) Co-ordinated ocular development from human iPS cells and recovery of corneal function. *Nature* 531: 376–380. <https://doi.org/10.1038/nature17000> PMID: 26958835
27. Mikhailova A, Ilmarinen T, Uusitalo H, Skottman H (2014) Small-molecule induction promotes corneal epithelial cell differentiation from human induced pluripotent stem cells. *Stem Cell Reports* 2: 219–231. <https://doi.org/10.1016/j.stemcr.2013.12.014> PMID: 24527395
28. Sakurai M, Hayashi R, Kageyama T, Yamato M, Nishida K (2011) Induction of putative stratified epithelial progenitor cells in vitro from mouse-induced pluripotent stem cells. *J Artif Organs* 14: 58–66. <https://doi.org/10.1007/s10047-010-0547-3> PMID: 21298309
29. Ludwig TE, Bergendahl V, Levenstein ME, Yu J, Probasco MD, Thomson JA. (2006) Feeder-independent culture of human embryonic stem cells. *Nat Methods* 3: 637–646. <https://doi.org/10.1038/nmeth902> PMID: 16862139
30. Calderon-Gierszal EL, Prins GS (2015) Directed Differentiation of Human Embryonic Stem Cells into Prostate Organoids In Vitro and its Perturbation by Low-Dose Bisphenol A Exposure. *PLoS One* 10: e0133238. <https://doi.org/10.1371/journal.pone.0133238> PMID: 26222054
31. Jeon JH, Suh HN, Kim MO, Han HJ (2013) Glucosamine-induced reduction of integrin beta4 and plectin complex stimulates migration and proliferation in mouse embryonic stem cells. *Stem Cells Dev* 22: 2975–2989. <https://doi.org/10.1089/scd.2013.0158> PMID: 23815613
32. Shi L, Yu X, Yang H, Wu X (2013) Advanced glycation end products induce human corneal epithelial cells apoptosis through generation of reactive oxygen species and activation of JNK and p38 MAPK pathways. *PLoS One* 8: e66781. <https://doi.org/10.1371/journal.pone.0066781> PMID: 23776698
33. Chang CY, McGhee JJ, Green CR, Sherwin T (2011) Comparison of stem cell properties in cell populations isolated from human central and limbal corneal epithelium. *Cornea* 30: 1155–1162. <https://doi.org/10.1097/ICO.0b013e318213796b> PMID: 21849892
34. Huang M, Li N, Wu Z, Wan P, Liang X, Zhang W, et al. (2011) Using acellular porcine limbal stroma for rabbit limbal stem cell microenvironment reconstruction. *Biomaterials* 32: 7812–7821. <https://doi.org/10.1016/j.biomaterials.2011.07.012> PMID: 21784513
35. Du L, Wu X, Pang K, Yang Y (2011) Histological evaluation and biomechanical characterisation of an acellular porcine cornea scaffold. *Br J Ophthalmol* 95: 410–414. <https://doi.org/10.1136/bjo.2008.142539> PMID: 20956275
36. Pang K, Du L, Wu X (2010) A rabbit anterior cornea replacement derived from acellular porcine cornea matrix, epithelial cells and keratocytes. *Biomaterials* 31: 7257–7265. <https://doi.org/10.1016/j.biomaterials.2010.05.066> PMID: 20598368
37. Gonzalez S, Mei H, Nakatsu MN, Baclagon ER, Deng SX (2016) A 3D culture system enhances the ability of human bone marrow stromal cells to support the growth of limbal stem/progenitor cells. *Stem Cell Res* 16: 358–364. <https://doi.org/10.1016/j.scr.2016.02.018> PMID: 26896856
38. Chen B, Mi S, Wright B, Connon CJ (2010) Investigation of K14/K5 as a stem cell marker in the limbal region of the bovine cornea. *PLoS One* 5: e13192. <https://doi.org/10.1371/journal.pone.0013192> PMID: 20949137

39. Selver OB, Barash A, Ahmed M, Wolosin JM (2011) ABCG2-dependent dye exclusion activity and clonal potential in epithelial cells continuously growing for 1 month from limbal explants. *Invest Ophthalmol Vis Sci* 52: 4330–4337. <https://doi.org/10.1167/iov.10-5897> PMID: 21421882
40. Kurpakus MA, Stock EL, Jones JC (1990) Expression of the 55-kD/64-kD corneal keratins in ocular surface epithelium. *Invest Ophthalmol Vis Sci* 31: 448–456. PMID: 1690687
41. Barnard Z, Apel AJ, Harkin DG (2001) Phenotypic analyses of limbal epithelial cell cultures derived from donor corneoscleral rims. *Clin Experiment Ophthalmol* 29: 138–142. PMID: 11446453
42. Nichols J, Zevnik B, Anastassiadis K, Niwa H, Klewe-Nebenius D, Chambers I, et al. (1998) Formation of pluripotent stem cells in the mammalian embryo depends on the POU transcription factor Oct4. *Cell* 95: 379–391. PMID: 9814708
43. Schlotzer-Schrehardt U, Kruse FE (2005) Identification and characterization of limbal stem cells. *Exp Eye Res* 81: 247–264. <https://doi.org/10.1016/j.exer.2005.02.016> PMID: 16051216
44. Priya CG, Prasad T, Prajna NV, Muthukkaruppan V (2013) Identification of human corneal epithelial stem cells on the basis of high ABCG2 expression combined with a large N/C ratio. *Microsc Res Tech* 76: 242–248. <https://doi.org/10.1002/jemt.22159> PMID: 23280693
45. Shipley GD, Pittelkow MR (1987) Control of growth and differentiation in vitro of human keratinocytes cultured in serum-free medium. *Arch Dermatol* 123: 1541a–1544a. PMID: 2445299
46. Tsao MC, Walthall BJ, Ham RG (1982) Clonal growth of normal human epidermal keratinocytes in a defined medium. *J Cell Physiol* 110: 219–229. <https://doi.org/10.1002/jcp.1041100217> PMID: 7040427
47. Yasumoto S, Kunimura C, Kikuchi K, Tahara H, Ohji H, Yamamoto H, et al. (1996) Telomerase activity in normal human epithelial cells. *Oncogene* 13: 433–439. PMID: 8710384
48. Geerling G, Daniels JT, Dart JK, Cree IA, Khaw PT (2001) Toxicity of natural tear substitutes in a fully defined culture model of human corneal epithelial cells. *Invest Ophthalmol Vis Sci* 42: 948–956. PMID: 11274071
49. Loureiro RR, Cristovam PC, Martins CM, Covre JL, Sobrinho JA, Ricardo JR, et al. (2013) Comparison of culture media for ex vivo cultivation of limbal epithelial progenitor cells. *Mol Vis* 19: 69–77. PMID: 23378720
50. Nandadasa S, Tao Q, Menon NR, Heasman J, Wylie C (2009) N- and E-cadherins in *Xenopus* are specifically required in the neural and non-neural ectoderm, respectively, for F-actin assembly and morphogenetic movements. *Development* 136: 1327–1338. <https://doi.org/10.1242/dev.031203> PMID: 19279134
51. Resende RR, da Costa JL, Kihara AH, Adhikari A, Lorencon E (2010) Intracellular Ca²⁺ regulation during neuronal differentiation of murine embryonal carcinoma and mesenchymal stem cells. *Stem Cells Dev* 19: 379–394. <https://doi.org/10.1089/scd.2008.0289> PMID: 19032055
52. Cummins EP, Oliver KM, Lenihan CR, Fitzpatrick SF, Bruning U, Scholz CC, et al. (2010) NF-kappaB links CO₂ sensing to innate immunity and inflammation in mammalian cells. *J Immunol* 185: 4439–4445. <https://doi.org/10.4049/jimmunol.1000701> PMID: 20817876
53. Khoshnan A, Patterson PH (2012) Elevated IKKalpha accelerates the differentiation of human neuronal progenitor cells and induces MeCP2-dependent BDNF expression. *PLoS One* 7: e41794. <https://doi.org/10.1371/journal.pone.0041794> PMID: 22848609
54. Obata S, Goi T, Nakazawa T, Kimura Y, Katayama K, Yamaguchi A. (2013) Changes in CO₂ concentration increase the invasive ability of colon cancer cells. *Anticancer Res* 33:1881–5. PMID: 23645734
55. Hamad M, Irhimeh MR, Abbas A. (2016) Hypercapnia slows down proliferation and apoptosis of human bone marrow promyeloblasts. *Bioprocess Biosyst Eng* 39:1465–75. <https://doi.org/10.1007/s00449-016-1624-7> PMID: 27194031
56. Huang M, Wang B, Wan P, Liang X, Wang X, Liu Y, et al. (2015) Roles of limbal microvascular net and limbal stroma in regulating maintenance of limbal epithelial stem cells. *Cell Tissue Res* 359:547–63. <https://doi.org/10.1007/s00441-014-2032-4> PMID: 25398719
57. Ohta S, Imaizumi Y, Okada Y, Akamatsu W, Kuwahara R, Ohyama M, et al. (2011) Generation of Human Melanocytes from Induced Pluripotent Stem Cells. *PLoS One* 6: e16182. <https://doi.org/10.1371/journal.pone.0016182> PMID: 21249204
58. Takahashi K, Yamanaka S. (2006) Induction of pluripotent stem cells from mouse embryonic and adult fibroblast cultures by defined factors. *Cell* 126:663–76. <https://doi.org/10.1016/j.cell.2006.07.024> PMID: 16904174
59. Robinton Daisy A., Daley George Q. (2012) The promise of induced pluripotent stem cells in research and therapy. *Nature* 481: 295–305. <https://doi.org/10.1038/nature10761> PMID: 22258608